Cooperative taming of CS_2/oxetane copolymerisation: Consequences of main-chain sulfuration on polymer properties and catalysis

Christoph Fornacon-Wood,[a] Cesare Gallizioli,[a] Merlin R. Stühler,[a] Carsten Müller,[a] Patrick Pröhm,[a]
Alex J. Plajer [a,*]

[a] Intitut für Chemie und Biochemie., Freie Universität Berlin, Fabeckstraße 34-36, 14195 Berlin; *email: plajer@zedat.fu-berlin.de. Key words: ring-opening (co)polymerisation, sulfur containing polymers, cooperative catalysis, degradable polymers, depolymerization.

Abstract: CS_2 promises easy access to degradable sulfur-rich polymers and insights into how main-group derivatisation affects polymer formation and properties, though its ring-opening copolymerisation is plagued by low linkage selectivity and small-molecule by-products. We demonstrate that a cooperative Cr(III)/K catalyst selectively delivers poly(dithiocarbonates) from CS_2 and oxetanes while state-of-the-art strategies produce linkage scrambled polymers and heterocyclic by-products. The formal introduction of sulfur centres into the parent polycarbonates results in a net shift of the polymerisation equilibrium towards, and therefore facilitating, depolymerisation. During copolymerisation however the catalyst enables near quantitative generation of the metastable polymers in high sequence selectivity by limiting the lifetime of alkoxide intermediates. Furthermore, linkage selectivity is key to obtain semi-crystalline materials that can be moulded into self-standing objects. Our report demonstrates the potential of cooperative catalysis to produce previously inaccessible main-group rich materials with beneficial chemical and physical properties

Introduction

The incorporation of sulfur centres into the polymer main chain rationally offers distinct material properties and functions associated with the periodic trends of the main-group elements.[1] The altered electronic nature of sulfur containing polymers compared to their lighter oxygen analogues causes amongst others degradability benefits, the potential to scavenge heavy metal contaminants, high refractive indices, stimuli responsiveness in drug delivery systems and enhanced semi-crystallinity.[2–7] Moving from oxygenated to sulfurated polymers can furthermore be used to tune the (de)polymerisation equilibria of polymers to facilitate chemical polymer recling.[8–10] Furthermore, using monomers which can be directly sourced from elemental sulfur (such as CS_2 from S_8 and methane) is also relevant in the context of S_8 utilization, a waste product of the petrochemical industry being produced at an annual megaton surplus.[11–15] Sulfur containing polymers are often synthesized by condensation or ring-opening polymerisation (ROP) methods, which can require multi-step monomer synthesis and do not give easy access to many polymer structures.[16,17] An increasingly popular method for the synthesis of heteroatom containing polymers is the ring-opening copolymerisation (ROCOP) of a strained heterocycle with heteroallenes. Having gained prominence for the selective copolymerisation of CO_2 with epoxides or oxetanes to polycarbonates, ROCOP cannot only make use of under-utilized monomer feedstocks but also produce previously inaccessible polymer structures.[18–22] Taking this methodology to the arena of sulfurated polymers, ROCOP of carbonyl sulfide COS with epoxides or oxetane represents a well-established route to selectively yield poly(monothiocarbonates) (**Figure 1(a)**).[23–29] Yet this ROCOP requires specialised steel reactor set-ups to safely handle highly toxic, flammable and gaseous carbonyl sulfide as well as commercial access to high purity COS (which is for example currently not the case in Europe) limiting the utility of this ROCOP in standard research laboratories.

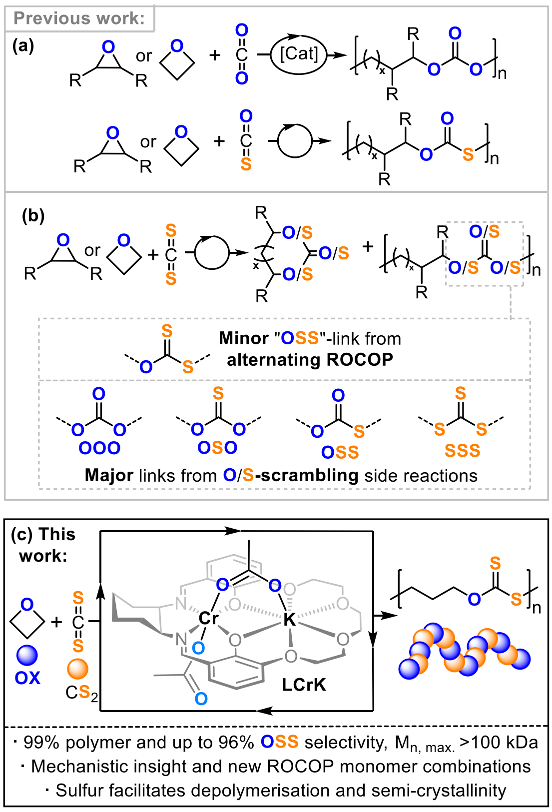

Figure 1: Comparison of products formed during (a) (CO_2 or COS)/(epoxide or oxetane) and (b) CS_2/(epoxide or oxetane) ROCOP. (c) Selective CS_2/oxetane ROCOP yielding poly(dithiocarbonates) presented in this report. x = 0 (R = H) ,1 (R = H, alkyl).

Using the liquid heavier homologue CS_2 is substantially simpler as it can be employed as a cosolvent and in principle allows access to copolymers with even higher sulfur ranks. However, the ROCOP of CS_2 with oxygen containing heterocycles has so far been plagued with numerous side reactions as show in **Figure 1(b)**. Polymers comprising different mono- (-O-C(=S)-O- **OSO**, O-C(=O)-S- **OOS**), di- (-O-C(=S)-S- **OSS**) and trithiocarbonate (-S-C(=S)-S- **SSS**) as well as all-oxygen carbonate (-O-C(=O)-O- **OOO**) and thioether links are always obtained in addition to small molecule by-products, such as different cyclic (thio)carbonates, thiiranes and COS instead of the expected poly(dithiocarbonates) from alternating ROCOP as demonstrated, assigned and rationalised by the groups of Wan, Zhang and Darensbourg.[30–38] Polymer selectivities versus cyclic heterocarbonates range from 30 to 80% in which dithiocarbonate links from alternating copolymerisation make up the minor (typically 0 – 30 %) fraction. Product distribution and polymer composition strongly depend on the exact reaction conditions making material properties unpredictable and necessitating time-consuming purification steps. The process behind the formation of the different linkages has been termed O/S-scrambling and is suspected to originate from the attack of metal-alkoxide chain-ends (formed from epoxide/oxetane ring-opening alike intermediate **A** in **Figure 2**) into dithiocarbonate linkages in place of propagation with CS_2 (forming metal-dithiocarbonate chain ends alike **DTC** in **Figure 2**). Notably this side-process extends to related polymerisations and causes linkage scrambling and small molecule by-products.[39–46] Previously it has been shown for all-oxygen ROCOP that cooperative catalysts can control the reactivity of alkoxide intermediates and limit or even productively regulate side reactions.[47–54] Williams and co-workers in particular showed that a heterobimetallic Co(III)K catalyst can limit back-biting side reactions originating form alkoxides in CO_2/epoxide ROCOP which lead to excellent polymer and linkage selectivities.[55] Therefore such catalysts could potentially also limit the O/S scrambling process starting from alkoxide intermediates thus enabling selective CS_2 ROCOP (**Figure 1(c)**). We hypothesized that oxetane (OX) are particularly interesting comonomers as previous reports by Darensbourg and Zhang showed that sulfur enhances semi-crystallinity is observed in the COS/OX copolymers.[28] The same was not the case for the CS_2/OX copolymers which we inferred to stem from the uncontrolled microstructure of this polymer as a consequence of the O/S scrambling process.[34] Hence this monomer combination represents an opportunity for selective catalysis to potentially control polymer properties which we report in this contribution.

Results and Discussion

Motivated by the precedence for chromium(III)-salen catalysts in CS_2/oxetane (CS_2/OX) ROCOP and work on potassium based systems within heterobinucleating ligands alike **L**, a heterobimetallic Cr(III)/K complex **LCrK** was prepared by one-pot template condensation of **L**H_2 with diamino-cyclohexane, KOAc and $Cr(OAc)_2$ following aerobic oxidation (see ESI Section S2).[34,55,56] The complex was obtained as the water adduct **LCrK**·H_2O and characterised by elemental analysis, IR spectroscopy and HR-ESI mass spectrometry. Testing **LCrK** at previously optimized reaction conditions (1 eq. catalyst: 1000 eq OX: 2000 eq. CS_2 and 80ºC, **Table 1** run#1, **Figure 2**, ESI Section S3) in a melamin capped vial with a teflon inlay yielded a highly viscous product mixture in which stirring stopped after 2 h.[34,35,39] Cooling to RT caused solidification via spherulite formation as seen by optical microscopy. Analysis of the product mixture by ^1H NMR spectroscopy reveals 99% formation of poly(heterocarbonate), only trace amounts of small molecule by-products and no evidence of homopolymer links (ESI Section S4).

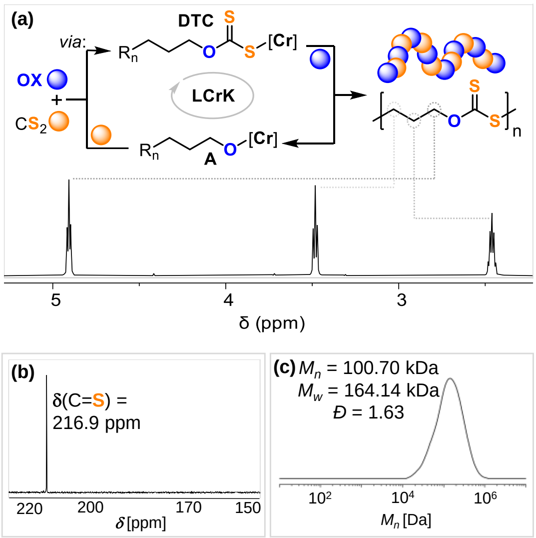

Figure 2: (a) CS_2/OX ROCOP scheme and ^1H ($CDCl_3$, 400 MHz), (b) ^{13}C ($CDCl_3$, 126 MHz) NMR as well as (c) SEC trace of the isolated polymer corresponding to **Table 1** run #1. R_n denotes growing polymer chain.

Table 1: CS_2/OX ROCOP with **LCrK**.

Run	**Cat:OX:CS$_2$**	**T [º]**	**t [h]^c**	**TON^a**	**OSS [%]^b**	**M_n,[kDa] (Đ)^c**
#1	1:1000:2000	80	2	820	96	14.03 (1.32)
#2	1:1000:1000	80	1.5	930	86	17.04 (2.23)
#3	1:1000:4000	80	2	950	95	15.66 (1.75)
#4	1:1000:2000	40	24	400	96	5.20 (1.37)
#5	1:1000:2000	60	20	1000	95	14.23 (1.84)

#6	1:1000:2000	90	0.75	750	94	11.62 (1.40)
#7	1:1000:2000	110	0.25	980	88	13.26 (1.75)
#8	1:4000:8000	80	2	3800	96	79.88 (1.67)
#9	1:10^4:2x10^4	80	4	7300	96	100.70 (1.63)
#Lit. [34]*	1:1000:2000	80	12	1000	6	6.50 (1.76)

Note that for run #1-#9 99% polymer selectivity is observed; in the case of the literature report run #Lit [34] only 64% polymer selectivity was observed. [a] Turnover number (TON), number of equivalents of OX consumed per equivalent of catalyst. [b] Relative integrals, in the normalised ^{1}H NMR spectrum of CH_2 resonances due OSS versus other heterocarbonate links. [c]Determined by GPC (gel permeation chromatography) measurements conducted in THF, using narrow MW polystyrene standards to calibrate the instrument. $M_{n,theor.}$= 27 - 978 kDa.

The polymer can be easily isolated by centrifugation and air drying and is obtained as a pale-yellow powder (M_n = 14.03 kg/mol, $Đ$ = 1.32). It comprises ca. 96% **OSS** links (d(C^q=S) = 216.9 ppm, $\tilde{\nu}$(C=S) = 1036.1 cm^{-1}) and 4% scrambled links as quantified by ^{1}H NMR spectroscopy. Such high selectivity represents a significant improvement over state-of-the-art catalysis which produces cyclic heterocarbonate by-products (36%) and polymers only comprising 6% **OSS** links under the same conditions (**Table 1** run #Lit.). To explore our new methodology further, we next assessed the effects of different reaction conditions and again observed 99% polymer formation in all cases. As seen in **Table 1** lower CS_2 loadings lead to more O/S-scrambling while higher CS_2 loadings do not improve the **OSS** selectivity (run #2, #3). Therefore, we continued our study with a 1:2 OX:CS_2 ratio to maximize selectivity but avoid excessive dilution (*vide infra*). Rates increase with temperature (maximum TOF of 3920 h^{-1} at 110 ºC), while **OSS** selectivity decreases with increasing temperature indicating that O/S scrambling is a thermodynamically favourable process. Furthermore, **LCrK** shows excellent performance (max. TON 7300) and activity at loadings as low as 0.003 mol% versus liquid monomers (run #9) producing polymers with a high maximum M_n = 100.70 kDa ($Đ$ = 1.63). State-of-the-art catalysis previously only achieved a high maximum M_n = 13.7 kDa (Đ = 1.70).[34] Although obtained molecular weights correlate to some extent with catalyst loadings (i.e. lower loading resulting in higher M_n) and M_n increase with reaction progress, theoretical and obtained molecular weight deviate, presumably due to chain transfer events (i.e. with water in the catalyst itself and protic impurities in the monomers), cyclic polymer formation and other side reactions as often observed in related polymerisations.[18,46,57] Attempts to obtain MALDI-MS data only results in polymer decomposition as reported for other sulfur-rich polymers.[13,42,45] Nevertheless, **LCrK** reliably produces high **OSS** and polymer selectivities, which raises the question whether this is due to favourable electronic matching of the employed metals evoking cooperativity or due to the circumstance that a single-component system is employed. Shedding light on this question (ESI Section S5, **Table 2**, **Figure 3**) we prepared the Na (**LCrNa**) and Rb (**LCrRb**) derivative and employed them in CS_2/OX ROCOP (**Table 2**, run #1 and #2). While **LCrRb** performs similar to **LCrK**, the sodium derivative **LCrNa** produces more scrambled (30%, primarily **SSS**) links and also substantial amounts (ca. 20%) of cyclic carbonate by-products. Selection of the transition metal is equally vital as moving to **LZnK** (run #3) featuring Zn(II), a popular metal in ROCOP catalysis, while keeping the active K results in no activity.[52,58,59]

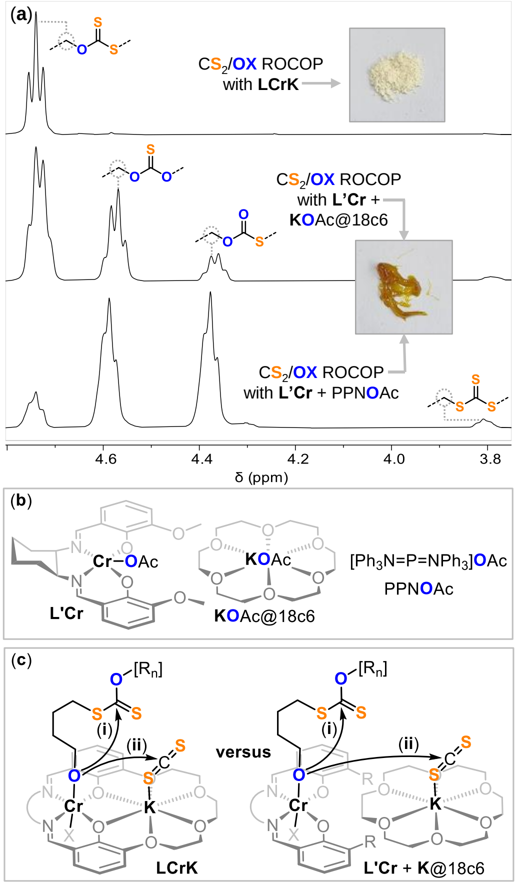

Figure 3: (a) Zoom into the ^{1}H NMR ($CDCl_3$, 400 MHz) spectra of crude mixtures produced by the monocomponent **LCrK** catalyst (**Table 1** run #1) and bicomponent variants (**Table 2** run #4 and #7) alongside photographs of the produced polymers. (b) Structures of other catalysts. **(c)** reaction pathways of propagation versus O/S scrambling for mono and bicomponent catalysts, X= OAc, [R_n] = polymer chain.

To mimic the electronic and coordinative situation in **LCrK** albeit as distinct components, we then employed a bicomponent catalyst comprising a bis-methoxy substituted $(MeO)_2$SalCyCrOAc **L'Cr** complex (**Figure 3**) with KOAc@18-crown-6. This led to a significant increase of scrambled links from 4% to 47% (**Table 2**, run #4) alongside 20%

cyclic carbonate by-products. While KOAc@18-crown-6 by itself is completely inactive (run #5), **L'Cr** by itself produces even more scrambled polymers (8% OSS links, run #6). Using **L'Cr** with PPNOAc, in which the cocatalytic salt features the weakly coordinating bis(triphenylphosphine)iminium cation, results in 90% scrambling and 20% cyclic carbonate by-products (run #7) suggesting that weakly coordinated chain-ends are responsible for low linkage selectivities. Interestingly, no crystallisation from solution is observed for these scrambled polymers which are obtained as amorphous semi-solids (*vide infra* for further discussion). It has been previously suggested that side-reactions originating from alkoxide intermediates are responsible for the scrambling process.[33–35] Hence, we reacted preformed poly(dithiocarbonate) (100 eq. repeat unit, **Table 1** run #1) with **LCrK** (1 eq.) and OX (1000 eq.), conditions under which due to the absence of CS_2 only alkoxide intermediates can exist, and indeed observed scrambling of the polymer (from 6% to 90% after 24h at 80ºC). Combined our results outlined in this paragraph indicate that **LCrK** supresses side reactions originating from decoordinated alkoxide chain ends via metal-metal cooperativity. Matching of the correct metals as well as ensuring cooperativity by fixing both active metals within the same ligand scaffold are vital to achieve high sequence selectivity in CS_2/OX ROCOP. As depicted in **Figure 3**(c) we infer in reference to recent computational studies by Williams and co-workers on CO_2/epoxide ROCOP that alkoxide based reactions originate from chromate centres while heteroallene activation occurs at the alkali metal.[56] Considering that reaction step (i) represents the entry point to O/S scrambling pathways (ESI Section S10) in reference to Darensbourg and Werner it becomes clear that if both metals are not fixed within the same scaffold the intermolecular propagation pathway (i) has to compete with the intramolecular scrambling pathway (ii) and the same is the conceptually the case for other bicomponent catalysts.[33–35] Heterobimetallic **LCrK** is hence inferred to lead to intermolecular propagation (i) and thereby avoid O/S scrambling.

Table 2: CS_2/OX ROCOP with alternative catalysts.

Run	Cat	t [h][c]	TON [a]	OSS [%][b]	**M_n,[kDa] (Đ)**[c]
#0	**LCrK**	2	820	96	14.03 (1.32)
#1	**LCrRb**	1.5	980	94	15.82 (1.62)
#2	**LCrNa**	17	1000	70	12.16 (1.91)
#3	**LZnK**	24	-	-	-
#4	**L'Cr + KOAc@ 18c6**	24	1000	47	12.41 (1.70)
#5	**KOAc@ 18c6**	24	-	-	-
#6	**L'Cr**	24	470	8	8.32 (1.81)
#7	**L'Cr + PPNOAc**	24	950	8	11.66 (1.78)

T = 80 ºC. Note that for run #0, #1 and #6 99% polymer selectivity is observed, while for run #2, #4 and #7 only ca. 80% polymer selectivity is observed. [a] Turnover number (TON), number of equivalents of OX consumed per equivalent of catalyst. [b] Relative integrals, in the normalised ^{1}H NMR spectrum of CH_2 resonances due OSS versus other heterocarbonate links. [c] Determined by GPC (gel permeation chromatography) measurements conducted in THF, using narrow MW polystyrene standards to calibrate the instrument. $M_{n,theo.}$= 63 - 131 kDa

Next, we investigated the monomer scope of our new methodology (ESI Section S6-S8) and found that **LCrK** is also capable of copolymerising a variety of previously unexplored monomer combination in quantitative polymer selectivity. The 3,3'-disubstituted oxetanes (**Table 3**, run #1 - #4, **Figure 4**) 3,3'-dimethyloxetane (OX^{Me}) as well as the ethyl (OX^{OEt}), benzyl (OX^{OBn}) and allylether (OX^{OAll}) substituted methyloxetane undergo CS_2 ROCOP yielding polymers with alkylic, arylic and functional olefine substituents. **OSS** selectivities are somewhat decreased compared to the parent CS_2/OX ROCOP (83-91% vs 96%) and in all cases errors comprise in equal parts of **SSS** linkages and **OSO** linkages. This can be rationalised by chain-end O/S exchange processes producing **OSO**-*alt*-**SSS** links as proposed by Werner and co-workers for CS_2/epoxide ROCOP (Scheme S17).[35] Note that this scrambling mode is distinct from the random scrambling observed in **Table 2**, for which random rather than equal ratios of the **OSO** and **SSS** are observed. Testing **LCrK** in CS_2 ROCOP of the ubiquitous epoxide Cylcohexeneoxide (CHO) also shows field leading performance (**Table 3**, run #5). 83% **OSS** links alongside a random distribution of combined 17% SSS, OSO, OOS and OOO links are observed. In contrast to CS_2/OX ROCOP, CS_2/CHO ROCP produces ca 20% cylic dithiocarbonate byproducts. Nevertheless **LCrK** also outperforms previously reported CS_2 /CHO catalysts which only achieves ca. 10% OSS linkages in 40-70% polymer selectivity.[32,35]

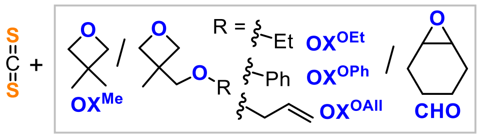

Figure 4: (a) Monomer combination undergoing ROCOP with **LCrK** corresponding to **Table 3.**

Table 3: Monomer scope of **LCrK.**

Run	Loading[a]	t [h]	TON [b]	Alt. [%][c]	M_n [kDa] (Đ)[d]	$T_{m/g/d,5\%}$
#0	1000 OX: 2000 CS_2	2	820	96	14.03 (1.32)	T_m = 89.3 ºC T_g = - 16.7 ºC T_d = 163.2 ºC
#1	1000 OX^{Me}: 2000 CS_2	24	1000	91	16.81 (1.53)	T_m = 107.2 ºC T_g = 5.5 ºC T_d = 195.0 ºC
#2	1000 OX^{OEt}: 2000 CS_2	30	1000	89	17.88 (1.43)	T_g = - 9.5 ºC T_d = 190.5 ºC
#3	1000 OX^{OBn}: 2000 CS_2	20	850	83	20.95 (1.54)	T_g = 8.0 ºC T_d = 208.0 ºC
#4	1000 OX^{OAll}: 2000 CS_2	1	1000	89	24.19 (1.58)	T_g = - 17.0 ºC T_d = 220.0 ºC
#5	1000 CHO: 2000 CS_2	8	600	83	15.94 (1.71)	T_g = 87.8 ºC T_d = 148.3 ºC

T = 80 ºC.[a] relative to 1 eq. **LCrK**. [b]Turnover number (TON), number of moles of OX consumed per mole of catalyst. [c] "Alternation selectivity": links resulting from formal alternation of the heteroallene/PTA with OX determined by comparing the relative integrals in the normalised ^1H NMR spectrum of CH_2 resonances adjacent to heteroatoms. [c]Determined by GPC (gel permeation chromatography) measurements conducted in THF, using narrow MW polystyrene standards to calibrate the instrument.

The circumstance that we observe 99% polymer selectivity irrespective of the employed reaction conditions (**Table 1**) or oxetane (**Table 3**) is surprising considering reports concerning the all-oxygen counterpart, i.e. CO_2/OX ROCOP.[60] Here, cyclic trimethylenecarbonate by-products are formed due to establishing (de)polymerisation equilibria between poly(trimethylenecarbonate) and the cyclic six-membered carbonates.[45,61–64] As this observation is most pronounced in geminally disubstituted derivatives due to the Thorpe-Ingold effect, we compared the relative energies of formation of the carbonate polymer carbonate **P** and the cyclic carbonate **C** from OX^{Me} and CO_2 as well as the alternating dithiocarbonate polymer $\mathbf{P^T}$ and the cyclic dithiocarbonates $\mathbf{C^T}$ from OX^{Me} and CS_2 on the B3LYP/cc-pVDZ level of theory (**Figure 5**(**a$_{1/2}$**)) with periodic boundary conditions for **P** and $\mathbf{P^T}$ (ESI Section S11), i.e. considering the energy of formation of one repeating unit in an infinite chain. As immediately apparent, CE_2/OX^{Me} coupling to either cyclic (ΔE = -61 kJ/mol for E = O and -103 kJ/mol for E = S) or poly(dithio)carbonate (ΔE = -116 kJ/mol for E = O and -148 kJ/mol for E = S) is more exergonic for CS_2 than for CO_2, a likely consequence of the decreased stability of a C=E bond versus two C-E bonds which are broken and formed the coupling process when moving from O to S.[65] In both cases the polymers **P** or $\mathbf{P^T}$ are more stable than the respective cyclic forms **C** or $\mathbf{C^T}$ reflecting *inter alia* the release of ring-strain energy upon polymerisation. However, polymer stability is more pronounced in the all-oxygen case (**Figure 5**(**a$_1$**), −55 kJ/mol moving from **C** to **P**) than in the sulfurated case (**Figure 5**(**a$_2$**), −45 kJ/mol moving from $\mathbf{C^T}$ to $\mathbf{P^T}$) which is surprising given the near quantitative polymer selectivity of our CS_2 ROCOP compared to previous CO_2 ROCOPs (*vide supra)* giving cyclic carbonate by-products due to equilibrium limitations.[62] Comparison of the bonding situation in the respective small molecules with the polymers (i.e. **C** with **P** and $\mathbf{C^T}$ with $\mathbf{P^T}$) shows near identical bonding orders in **C** and **P** as well as $\mathbf{C^T}$ and $\mathbf{P^T}$. This suggests that not electronic changes, but rather different ring strain energies of **C** and $\mathbf{C^T}$ are responsible for the differences in poly- versus cyclic (dithio)carbonate stability which we infer is due a greater tolerance towards bond-angle variation when moving down the periodic table.[66] Combined, these results imply that the (de)polymerisation equilibrium of the $\mathbf{P^T} \rightleftarrows \mathbf{C^T}$ copolymer must lie more on the cyclic (dithio)carbonate side then for the all-oxygen equilibrium $\mathbf{P} \rightleftarrows \mathbf{C}$ under identical conditions. In this respect *Endo* and co-workers reported that catalytic KO^tBu in THF reconstitutes equilibria states of isolated **P**, i.e. starting from 100% **P** at 0.45M in THF and 20 ºC resulted in 7% **C** and 93% **P** at equilibrium.[61] Subjecting isolated the CS_2/OX^{Me} copolymer $\mathbf{P^{T*}}$ (i.e. $\mathbf{P^T}$ with 92% **OSS** and 8% **OSO**-*alt*-**SSS** links; **Table 3**, run #1) to analogous conditions results in >99% depolymerisation into ca. 95% $\mathbf{C^T}$ and ca. 5% unidentified by-products and this confirms sulfur enhanced depolymerisability as predicted by DFT. Accordingly, our other CS_2/OX^{OR} polymers (**Table 3**, run #2 – #4) likewise undergo >99% depolymerisation under the above conditions into cyclic dithiocarbonates, while related polycarbonates show equilibrium limitations.[61,62] Note that depolymerisation results in some reversion of the O/S exchange process and reshuffles the O and S centres from the **OSO**-*alt*-**SSS** links into cyclic dithiocarbonates containing one O and two S atoms. The CS_2/OX copolymer likewise undergoes depolymerisation albeit necessitating higher dilution (0.023 M) for >99% depolymerisation. While depolymerisation of the nearly alternating copolymer (**Table 2**, run #0) forms cyclic dithiocarbonates in >95% selectivity, depolymerisation of the randomly scrambled copolymer (**Table 2**, #7) forms a complex inseparable mixture of products, highlighting the necessity for sequence control to enable selective depolymerisation. The KO^tBu catalysed (de)polymerisation mechanism has previously been proposed to involve alkoxide chain-ends that backbite into carbonates links during depropagation and attack into cyclic carbonate

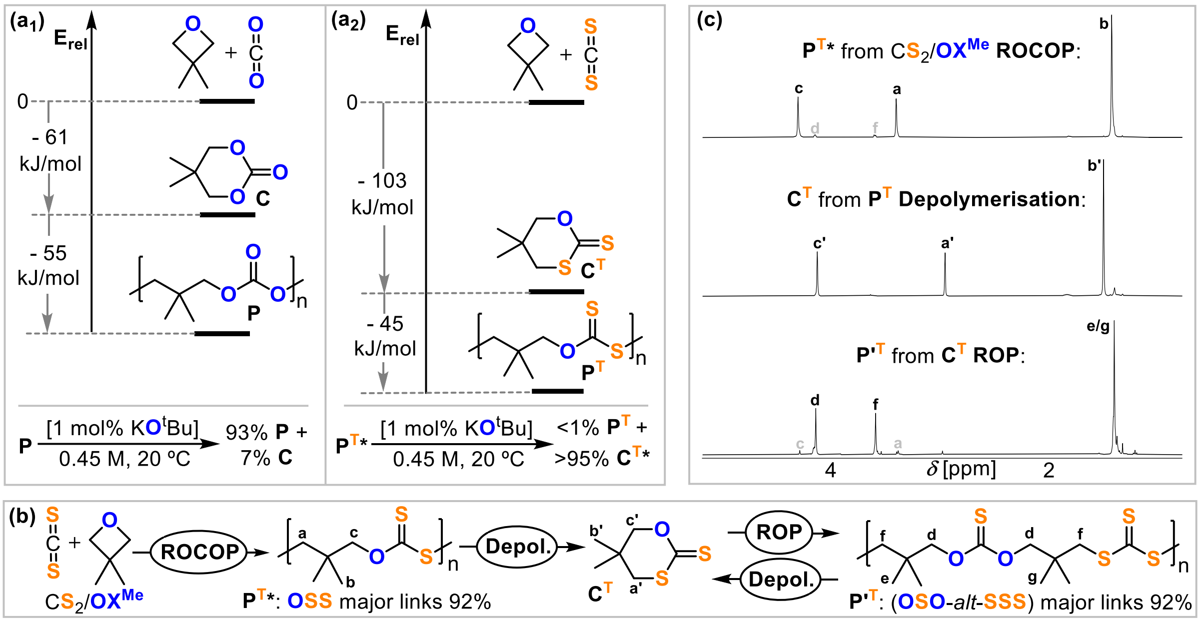

Figure 5: Relative energies on the B3LYP/cc-pVDZ level of theory of cyclic versus polymer formation for the (a$_1$) all-oxygen CO$_2$/OX^{Me} and (a$_2$) the sulfurated CS$_2$/OX^{Me} cases as well as experimentally determined (de)polymerisation equilibria states under specified conditions; all-oxygen carbonate data displayed in reference to Endo and co-workers.[61] *note that **P**^{T} as employed in the depolymerisation errors contains 8% OSO-*alt*-SSS errors; >99% depolymerisation products comprise of ca. 95% **C**^{T} and 5% unidentified by-products. (b) ROCOP into depolymerisation into ROP sequence. ROCOP conditions as per **Table 3** run #1; depolymerisation conditions as per (a); ROP conditions 1 eq. 1,5,7-triazabicyclo[4.4.0]dec-5-en (TBD): 1 BnOH: 100 eq. **C**^{T}, 4M in DCM, 20ºC, 16h, 45% conversion, obtained polymer **P'**^{T}: M_n = 4.50 kg/mol, $Đ$ = 1.22, $M_{n,theo}$ = 7.29 kg/mol. (c) Overlaid ^{1}H NMR spectra (400 MHz, CDCl$_3$, 25 ºC) of **P**^{T*} produced by CS$_2$/OX^{Me} ROCOP, **C**^{T} produced by depolymerisation and **P'**^{T} produced by **C**^{T} ROP.

monomers during propagation.[61] We probed this hypothesis by attempting to perform **P**^{T*} depolymerisation in a 1:1 THF:CS$_2$ mixture, in which metal-alkoxide chain-ends should insert CS$_2$ forming less nucleophilic metal-dithiocarbonate chain-ends and indeed did not find any depolymerisation to occur. In accordance with thermodynamically favoured depolymerisation, attempted ring-opening polymerisation of **C**^{T} at 0.45M in THF does not occur, conditions under which **C** undergoes polymerisation.[61] Nevertheless repolymerisation of **C**^{T} can be achieved by solvent choice and concentration. Increasing the concentration to 4M in DCM with a 1,5,7-triazabicyclo[4.4.0]dec-5-en (TBD) and BnOH catalyst (1 TBD: 1BnOH: 100 **C**^{T}, RT, 16 h) sufficiently shifts the (de)polymerisation equilibrium to achieve 45% ROP after 16 h (M_n = 4.50 kg/mol, $Đ$ = 1.22, $M_{n,theo}$ = 7.29 kg/mol) (**Figure 5**(**b/c**)). The ROP polymer **P'**^{T} comprises **OSO**-*alt*-**SSS** (92%) and **OSS** (8%) links, which can be rationalized by chain-end alkoxide originated O/S exchange processes in reference to related reports by Buchard and co-workers.[45,46] Similar to **P**^{T*} (T_m = 107.2 ºC T_g = 5.5 ºC), **P'**^{T} is semi-crystalline (T_m = 54.7 ºC T_g = -10.0 ºC) albeit with significantly lowered melting temperature by ca. 50ºC again highlighting how sequence selectivity achieved in the first place by **LCrK** enhances material properties. Subjecting **P'**^{T} to the depolymerisation conditions outlined above likewise results in >99% depolymerisation under reversion of the O/S exchange process yielding **C**^{T} highlighting the potential of our copolymers in the context of chemical recycling.[67] Taken together our results indicate that CS$_2$/OX ROCOP generates poly(dithiocarbonates) which are in a metastable or non-equilibrated state as a consequence of a sulfur induced ring-strain decrease. However, in ROCOP with **LCrK** metal-dithiocarbonate formation at the propagating chain-end with CS$_2$ limits the lifetime of metal-alkoxide intermediates which are responsible for establishing (de)polymerisation equilibria into cyclic dithiocarbonate and for O/S scrambling. This does not (efficiently) occur in other ROCOPs and ROPs targeting related poly(thio)carbonates which gives reasons behind the selectivity benefits of **LCrK** over existing methodologies. As mentioned above, the high linkage selectivity achieved by **LCrK** can have a strong influence on the thermal properties of the obtained polymers. The CS$_2$/OX copolymers with high **OSS** selectivity (i.e. **Table 1**) crystallise from the reaction mixture at room temperature and hence exhibits semi-crystallinity in the solid state as shown by DSC (T_m = 89.3 ºC, DH_m = 36.01 J/g, T_c = 47.0 ºC for **Table 1** run #1 in the 2nd DSC heating cycle, **Figure 6**) and PXRD (primary reflections are observed at θ = 19.7º, 22.13º and 27.54º). Neither solution nor solid-crystallisation in DSC measurements is observed for the O/S-scrambled polymers (**Table 2** run #4 -#7) which are obtained as amorphous materials after removal of excess monomers and do not exhibit any semi-crystallinity by DSC (T_g = -29.1 ºC for **Table 2** run #7). Owing to the low glass-transition temperature of these material, linkage selectivity is hence key to allow these materials to be hot pressed into free-standing and shape persistent films.

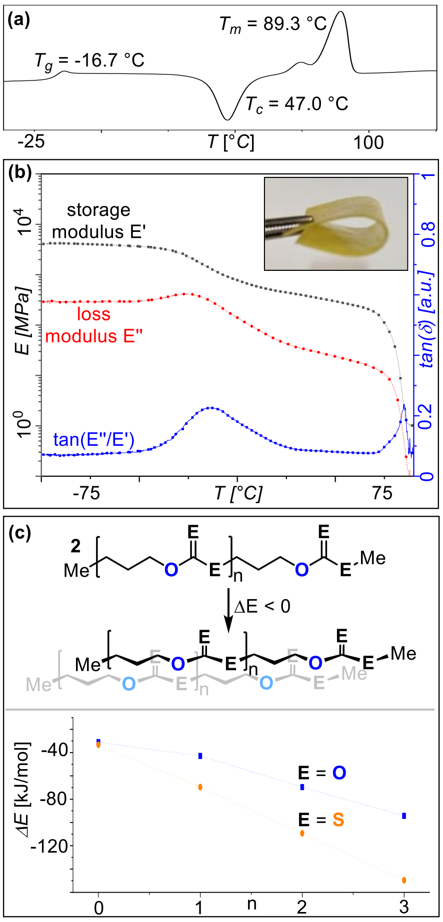

Figure 6: (a) DSC curve of the 2nd heating cycle for polymer corresponding to Table 1, run #1. (b) Overlay plots of storage modulus E′, loss modulus E″ and tanδ(E″/E′) for hot-pressed films (example photograph inlayed) with materials from Table 1 run #9 measured by DMA (tension film mode, 1 Hz, 1 °C per min). (c) Free energy release upon association of model oligomers assessed on the B3LYP/cc-pVDZ level of theory.

Uniaxial tensile testing on films prepared from the polymer corresponding to **Table 1** run #9 shows a break at 3.6% elongation and a tensile strength of 20.6 MPa. Furthermore, dynamic mechanical analysis (DMA) shows a thermomechanical spectrum typical of a semi-crystalline material. A high maximum storage modulus of E' = 4.2 GPa is observed in the glassy state which decreases to E' ≈ 0.7 - 0.3 GPa after an alpha glass transition at T_a = - 14.7ºC (defined as the maximum of tan(d), d = E''/E', **Figure 6**b) which corresponds well to the T_g observed by DSC. A rubbery plateau is observed until the flow temperature at about 85ºC is reached for the semi-crystalline poly(trimethylenedithiocarbonate). Note that the all-oxygen analogue poly(trimethylenecarbonate) obtained from CO_2/OX ROCOP has also been reported to be an amorphous material (T_g ~ -20 ºC).[63,68] Our results hence indicate that the selective incorporation of sulfur centres leads to tighter packing of polymer chains than in the all-oxygen case enabling semi-crystallinity and a regular polymer microstructure which is required to benefit from this effect. Although it has been previously reported that the formal substitution of sulfur for oxygen centres increases the crystallinity of polymers, the origins of this effect remain under debate.[69–71] Shedding light on the origin of crystallinity, we computationally assessed the intermolecular association between two molecules for a series of mono- to tetrameric Me[(CH$_2$)$_3$-O-C(=E)-E-]$_n$Me model dithiocarbonates (E = S) in comparison to the all-oxygen carbonate (E = O) counterparts (**Figure 6**, ESI Section S11). We chose linearly stretched conformations to maximize the interaction between the respective chains. In all cases, free energy optimisation results in face on association of the oligomers which maximizes the exposed surface area while minimizing the formation of hydrogen bonds or S⋯S contacts which have previously been suggested to cause sulfur-induced crystallinity.[32,69] AIM analysis reveals the absence of covalent interactions, indicating van-der-Waals forces to be the dominant form of attraction between chains. Attempted optimization of dimers without dispersion correction hence results in dissociation of the chains. Consequently, more polarisable sulfur centres should result in enhanced van-der-Waals interaction compared to the oxygen analogues. Accordingly, the association energy for dimerization decreases by ca. 25 kJ/mol on average per additional repeat unit n for E = O and by ca. 35 kJ/mol on average for E = S. Therefore, we suggest that increased interchain London dispersion contributes to sulfur induced semi-crystallinity in our systems. In comparison the COS/OX copolymer shows a significantly higher T_m of 133ºC (vs. 89.3ºC for the CS_2/OX copolymer) and enhanced hydrogen bonding interaction have been proposed to induce semi-crystallinity. Hence sulfur induced semi-crystallinity appears to arise through a combination of determinants exceeding the simple model outlined above.

Conclusions

In conclusion, we have demonstrated that moving from inter to intramolecularly cooperative catalysis unlocks the potential of CS_2 ROCOP to selectively yield sulfur-rich copolymers. Metal choice and proximity are responsible for limiting O/S scrambling side reactions that originate from metal-alkoxide chain-ends. The strategy also achieves the copolymerisation of previously unexplored monomer combinations yielding sulfur containing polymers from oxetanes. Moving from oxygen to sulfur renders our dithiocarbonates easier to depolymerise than the carbonate analogues as the produced heterocycle is less strained. Sequence selectivity is key to enable selective depolymerisation into dithiocarbonates and to obtain semi-crystalline materials to which increased interchain van der Waals interaction upon formal sulfuration contributes. Our report opens the door for the development of new main-group rich polymers with useful properties which were previously deemed inaccessible.

Acknowledgements

The VCI is acknowledged for a Liebig Fellowship for A. J. P. Prof. Dr. Christian Müller and Prof. Dr. Rainer Haag are thanked for continuous support and valuable discussions. ZEDAT is thanked for computational resources, Biosupramol and Dr. Günther Thiele (FU Berlin), Thomas Rybak and Prof. Dr. Bernhard Schartel (Bundesanstalt für Materialforschung Fachbereich 7.5) as well as Prof. Dr. Andreas Thünemann (Fachbereich 6.5) are thanked analytical support.

Conflict of Interest

There are no conflicts of interest.

Methods

Catalyst synthesis

Synthesis of **LCrK**·H_2O: Inside a nitrogen-filled glovebox KOAc (55 mg, 1 equiv.) was added to solution of the dialehyde precursor A (200 mg, 1 equiv., see ESI for preparation) in acetonitrile (10 mL) and the solution was stirred at room temperature for 30 min. Afterwards 1,2-diaminocyclohexane (64 mg, 1 equiv.) and $Cr(OAc)_2$ (95 mg, 1 equiv.) were added and the reaction mixture was stirred for a further 16 h at room temperature. The complex was oxidized by exposure to air and by the addition of acetic acid (60 µL, 2 equiv.) and the solution was stirred for 24 h open to air at room temperature. Afterwards the suspension was filtered, and all volatiles were in vacuum. The resulting solid was washed with Et_2O (2 x 50 mL) and dried in vacuo to afford **LCrK**·H_2O as a brown powder (319 mg, 82%). HRESI-MS positive mode: calculated [M - OAc]+ 616.1279. Found 616.1249. Elemental Analysis: calculated C 51.94 %, H 5.52 %, N 4.04 %; found C 51.81 %, H 5.70 %, N 4.29 %. Following the analogous procedure **LCrNa**·H_2O was prepared with NaOAc (46 mg) in 47% yield (HRESI-MS positive mode: calculated [M - OAc]+ 600.1540. Found 600.1542; Elemental Analysis **LCrNa**·H_2O: calculated C 53.18 %, H 5.65 %, N 4.13 %; found C 53.37 %, H 5.44 %, N 3.95 %) and **LCrRb**·H_2O was prepared with RbOAc (81 mg) in 54% yield (HRESI-MS positive mode: calculated [M - OAc]+ 662.0760. Found 662.0806; Elemental Analysis LCrRb·H2O: calculated C 48.69 %, H 5.18 %, N 3.79 %; found C 48.50 %, H 5.33 %, N 3.61 %).

Polymerisation protocol

Inside an argon filled glovebox, the catalyst, the monomers and an internal mesitylene standard were added to a flame dried vial equipped with a flame dried stirrer bar and sealed with a melamine cap containing a Teflon inlay. The vial was brought outside the glovebox and placed in a pre-heated aluminium block at the specified temperature for the specified time. At the specified end point of the reaction, the polymerisation mixture was cooled down to room temperature and extracted with $CDCl_3$ to determine the monomer conversion. The mixture was then added to 50 mL of MeOH and the polymer was isolated by centrifugation and dried in a vacuum oven set to 50 °C for 2 h. Alternatively the crude reaction mixture can also let cooled down to room temperature, causing the crystallisation of the polymer, which can then be isolated by centrifugation and air drying.

Bibliography

1. Steudel, R. *Elemental Sulfur and Sulfur-Rich Compounds II*. (Springer Science & Business Media, 2003).
2. Lee, T., Dirlam, P. T., Njardarson, J. T., Glass, R. S. & Pyun, J. Polymerizations with Elemental Sulfur: From Petroleum Refining to Polymeric Materials. *J. Am. Chem. Soc.* **144**, 5–22 (2022).
3. Crockett, M. P. *et al.* Sulfur-Limonene Polysulfide: A Material Synthesized Entirely from Industrial By-Products and Its Use in Removing Toxic Metals from Water and Soil. *Angew. Chem. Int. Ed.* **55**, 1714–1718 (2016).
4. Braatz, D. *et al.* Chemical Approaches to Synthetic Drug Delivery Systems for Systemic Applications. *Angew. Chem. Int. Ed.* doi:10.1002/anie.202203942 *(*2022),.
5. Li, H., Ollivier, J., Guillaume, S. M. & Carpentier, J.-F. Tacticity Control of Cyclic Poly(3-Thiobutyrate) Prepared by Ring-Opening Polymerization of Racemic β-Thiobutyrolactone. *Angew. Chem. Int. Ed.*, doi: 10.1002/anie.202202386 (2022).
6. Haider, T. P., Völker, C., Kramm, J., Landfester, K. & Wurm, F. R. Plastics of the Future? The Impact of Biodegradable Polymers on the Environment and on Society. *Angew. Chem. Int. Ed.* **58**, 50–62 (2019).
7. Yuan, P., Sun, Y., Xu, X., Luo, Y. & Hong, M. Towards high-performance sustainable polymers via isomerization-driven irreversible ring-opening polymerization of five-membered thionolactones. *Nat. Chem.* **14**, 294–303 (2022).
8. Wang, Y., Li, M., Chen, J., Tao, Y. & Wang, X. O-to-S Substitution Enables Dovetailing Conflicting Cyclizability, Polymerizability, and Recyclability: Dithiolactone vs. Dilactone. *Angew. Chem. Int. Ed.* **60**, 22547–22553 (2021).
9. Stellmach, K. A. *et al.* Modulating Polymerization Thermodynamics of Thiolactones Through Substituent and Heteroatom Incorporation. *ACS Macro Lett.* **11**, 895–901 (2022).
10. Shi, C. *et al.* High-performance pan-tactic polythioesters with intrinsic crystallinity and chemical recyclability. *Science Advances* **6**, eabc0495 (2020).

11. Tian, T., Hu, R. & Tang, B. Z. Room Temperature One-Step Conversion from Elemental Sulfur to Functional Polythioureas through Catalyst-Free Multicomponent Polymerizations. *J. Am. Chem. Soc.* **140**, 6156–6163 (2018).
12. Zhang, J. *et al.* Sulfur Conversion to Multifunctional Poly(O-thiocarbamate)s through Multicomponent Polymerizations of Sulfur, Diols, and Diisocyanides. *J. Am. Chem. Soc.* **143**, 3944–3950 (2021).
13. Ren, W.-M. *et al.* Controlled Disassembly of Elemental Sulfur: An Approach to the Precise Synthesis of Polydisulfides. *Angew. Chem. Int. Ed.* DOI: 10.1002/anie.202115950 (2022)
14. Jia, J. *et al.* Photoinduced inverse vulcanization. *Nat. Chem.* **14**, 1249–1257 (2022).
15. Kang, K.-S. *et al.* Sulfenyl Chlorides: An Alternative Monomer Feedstock from Elemental Sulfur for Polymer Synthesis. *J. Am. Chem. Soc.* doi:10.1021/jacs.2c10317 (2022).
16. Kausar, A., Zulfiqar, S. & Sarwar, M. I. Recent Developments in Sulfur-Containing Polymers. *Polym. Rev.* **54**, 185–267 (2014).
17. Zhang, X.-H. & Theato, P. *Sulfur-Containing Polymers: From Synthesis to Functional Materials*. (John Wiley & Sons, 2021).
18. Plajer, A. J. & Williams, C. K. Heterocycle/Heteroallene Ring-Opening Copolymerization: Selective Catalysis Delivering Alternating Copolymers. *Angew. Chem. Int. Ed.* doi: 10.1002/e202104495 (2022).
19. Longo, J. M., Sanford, M. J. & Coates, G. W. Ring-Opening Copolymerization of Epoxides and Cyclic Anhydrides with Discrete Metal Complexes: Structure–Property Relationships. *Chem. Rev.* **116**, 15167–15197 (2016).
20. Klaus, S., Lehenmeier, M. W., Anderson, C. E. & Rieger, B. Recent advances in CO2/epoxide copolymerization—New strategies and cooperative mechanisms. *Coord. Chem. Rev.* **255**, 1460–1479 (2011).
21. Lu, X.-B., Ren, W.-M. & Wu, G.-P. CO2 Copolymers from Epoxides: Catalyst Activity, Product Selectivity, and Stereochemistry Control. *Acc. Chem. Res.* **45**, 1721–1735 (2012).
22. Yang, G.-W., Zhang, Y.-Y. & Wu, G.-P. Modular Organoboron Catalysts Enable Transformations with Unprecedented Reactivity. *Acc. Chem. Res.* **54**, 4434–4448 (2021).
23. Yang, J.-L., Wu, H.-L., Li, Y., Zhang, X.-H. & Darensbourg, D. J. Perfectly Alternating and Regioselective Copolymerization of Carbonyl Sulfide and Epoxides by Metal-Free Lewis Pairs. *Angew. Chem. Int. Ed.* **56**, 5774–5779 (2017).
24. Yue, T.-J. *et al.* Facile Synthesis of Well-Defined Branched Sulfur-Containing Copolymers: One-Pot Copolymerization of Carbonyl Sulfide and Epoxide. *Angew. Chem. Int. Ed.* **59**, 13633–13637 (2020).
25. Yue, T.-J. *et al.* Synthesis of Chiral Sulfur-Containing Polymers: Asymmetric Copolymerization of meso-Epoxides and Carbonyl Sulfide. *Angew. Chem. Int. Ed.* **130**, 12852–12856 (2018).
26. Zhang, C.-J., Wu, H.-L., Li, Y., Yang, J.-L. & Zhang, X.-H. Precise synthesis of sulfur-containing polymers via cooperative dual organocatalysts with high activity. *Nat. Commun.* **9**, 2137 (2018).
27. Luo, M., Zhang, X.-H. & Darensbourg, D. J. Poly(monothiocarbonate)s from the Alternating and Regioselective Copolymerization of Carbonyl Sulfide with Epoxides. *Acc. Chem. Res.* **49**, 2209–2219 (2016).
28. Wu, H.-L. *et al.* Poly(trimethylene monothiocarbonate) from the Alternating Copolymerization of COS and Oxetane: A Semicrystalline Copolymer. *Macromolecules* **49**, 8863–8868 (2016).
29. Yue, T.-J. *et al.* Randomly Distributed Sulfur Atoms in the Main Chains of CO2-Based Polycarbonates: Enhanced Optical Properties. *Angew. Chem. Int. Ed.* **60**, 4315–4321 (2021).
30. Adachi, N., Kida, Y. & Shikata, K. Copolymerization of propylene oxide and carbon disulfide with diethylzinc–electron-donor catalyst. *J. Polym. Sci.: Polym. Chem. Ed.* **15**, 937–944 (1977).
31. Zhang, X.-H. *et al.* Atom-Exchange Coordination Polymerization of Carbon Disulfide and Propylene Oxide by a Highly Effective Double-Metal Cyanide Complex. *Macromolecules* **41**, 1587–1590 (2008).
32. Darensbourg, D. J., Andreatta, J. R., Jungman, M. J. & Reibenspies, J. H. Investigations into the coupling of cyclohexene oxide and carbon disulfide catalyzed by (salen)CrCl. Selectivity for the production of copolymers vs. cyclic thiocarbonates. *Dalton Trans.* 8891–8899 (2009).
33. Darensbourg, D. J., Wilson, S. J. & Yeung, A. D. Oxygen/Sulfur Scrambling During the Copolymerization of Cyclopentene Oxide and Carbon Disulfide: Selectivity for Copolymer vs Cyclic [Thio]carbonates. *Macromolecules* **46**, 8102–8110 (2013).
34. Luo, M., Zhang, X.-H. & Darensbourg, D. J. An Investigation of the Pathways for Oxygen/Sulfur Scramblings during the Copolymerization of Carbon Disulfide and Oxetane. *Macromolecules* **48**, 5526–5532 (2015).
35. Diebler, J., Komber, H., Häußler, L., Lederer, A. & Werner, T. Alkoxide-Initiated Regioselective Coupling of Carbon Disulfide and Terminal Epoxides for the Synthesis of Strongly Alternating Copolymers. *Macromolecules* **49**, 4723–4731 (2016).

36. Yang, J.-L. *et al.* Enabling Oxygen–Sulfur Exchange Reaction to Produce Semicrystalline Copolymers from Carbon Disulfide and Ethylene Oxide. *Macromol. Rapid Commun.* **42**, 2000472 (2021).
37. Yang, J.-L., Hu, L.-F., Cao, X.-H., Wang, Y. & Zhang, X.-H. An Investigation on the Production of Random Copolymer with Monothiocarbonate and Trithiocarbonate Units over Cyclic Thiocarbonate via Metal-free Catalysis. *Chin. J. Chem.* **38**, 269–274 (2020).
38. McGuire, T. M. & Buchard, A. Polymers from sugars and CS2: ring opening copolymerisation of a D-xylose anhydrosugar oxetane. *Polym. Chem.* **12**, 4253–4261 (2021).
39. Nakano, K., Tatsumi, G. & Nozaki, K. Synthesis of Sulfur-Rich Polymers: Copolymerization of Episulfide with Carbon Disulfide by Using [PPN]Cl/(salph)Cr(III)Cl System. *J. Am. Chem. Soc.* **129**, 15116–15117 (2007).
40. Wang, L.-Y., Gu, G.-G., Yue, T.-J., Ren, W.-M. & Lu, X.-B. Semiaromatic Poly(thioester) from the Copolymerization of Phthalic Thioanhydride and Epoxide: Synthesis, Structure, and Properties. *Macromolecules* **52**, 2439–2445 (2019).
41. Wang, L.-Y. *et al.* Intramolecularly Cooperative Catalysis for Copolymerization of Cyclic Thioanhydrides and Epoxides: A Dual Activation Strategy to Well-Defined Polythioesters. *ACS Catal.* **10**, 6635–6644 (2020).
42. Rupf, S., Pröhm, P. & Plajer, A. J. Lithium achieves sequence selective ring-opening terpolymerisation (ROTERP) of ternary monomer mixtures. *Chem. Sci.* **13**, 6355–6365 (2022).
43. Silbernagl, D., Sturm, H. & Plajer, A. J. Thioanhydride/isothiocyanate/epoxide ring-opening terpolymerisation: sequence selective enchainment of monomer mixtures and switchable catalysis. *Polym. Chem.* **13**, 3981–3985 (2022).
44. Plajer, A. J. Sequence selective ring-opening terpolymerisation facilitates higher order switchable catalysis. *ChemCatChem* doi: 10.1002/cctc.202200867 (2022).
45. Hardy, C., Kociok-Köhn, G. & Buchard, A. UV degradation of poly(lactic acid) materials through copolymerisation with a sugar-derived cyclic xanthate. *Chem. Commun.* **58**, 5463–5466 (2022).
46. López-Vidal, E. M., Gregory, G. L., Kociok-Köhn, G. & Buchard, A. Polymers from sugars and CS2: synthesis and ring-opening polymerisation of sulfur-containing monomers derived from 2-deoxy-D-ribose and D-xylose. *Polym. Chem.* **9**, 1577–1582 (2018).
47. S, S., Min, J. K., Seong, J. E., Na, S. J. & Lee, B. Y. A Highly Active and Recyclable Catalytic System for CO2/Propylene Oxide Copolymerization. *Angew. Chem. Int. Ed.* **47**, 7306–7309 (2008).
48. Yang, G.-W. *et al.* Precision copolymerization of CO2 and epoxides enabled by organoboron catalysts. *Nat. Synth.* **1**, 892-901 (2022).
49. Yang, G.-W. *et al.* Pinwheel-Shaped Tetranuclear Organoboron Catalysts for Perfectly Alternating Copolymerization of CO2 and Epichlorohydrin. *J. Am. Chem. Soc.* **143,** 3455 - 3465 (2021).
50. Abel, B. A., Lidston, C. A. L. & Coates, G. W. Mechanism-Inspired Design of Bifunctional Catalysts for the Alternating Ring-Opening Copolymerization of Epoxides and Cyclic Anhydrides. *J. Am. Chem. Soc.* **141**, 12760–12769 (2019).
51. Plajer, A. J. & Williams, C. K. Heterotrimetallic Carbon Dioxide Copolymerization and Switchable Catalysts: Sodium is the Key to High Activity and Unusual Selectivity. *Angew. Chem. Int. Ed.* **60**, 13372–13379 (2021).
52. Plajer, A. J. & Williams, C. K. Heterotrinuclear Ring Opening Copolymerization Catalysis: Structure–activity Relationships. *ACS Catal.* **11**, 14819–14828 (2021).
53. Lehenmeier, M. W. *et al.* Flexibly Tethered Dinuclear Zinc Complexes: A Solution to the Entropy Problem in CO2/Epoxide Copolymerization Catalysis? *Angew. Chem. Int. Ed.* **52**, 9821–9826 (2013).
54. Nagae, H. *et al.* Lanthanide Complexes Supported by a Trizinc Crown Ether as Catalysts for Alternating Copolymerization of Epoxide and CO2: Telomerization Controlled by Carboxylate Anions. *Angew. Chem. Int. Ed.* **57**, 2492–2496 (2018).
55. Deacy, A. C., Moreby, E., Phanopoulos, A. & Williams, C. K. Co(III)/Alkali-Metal(I) Heterodinuclear Catalysts for the Ring-Opening Copolymerization of CO2 and Propylene Oxide. *J. Am. Chem. Soc.* **142**, 19150 – 19160 (2020).
56. Deacy, A. C., Phanopoulos, A., Lindeboom, W., Buchard, A. & Williams, C. K. Insights into the Mechanism of Carbon Dioxide and Propylene Oxide Ring-Opening Copolymerization Using a Co(III)/K(I) Heterodinuclear Catalyst. *J. Am. Chem. Soc.* **144**, 17929–17938 (2022).
57. Darensbourg, D. J. Chain transfer agents utilized in epoxide and CO2 copolymerization processes. *Green Chem.* **21**, 2214–2223 (2019).
58. Kissling, S. *et al.* Dinuclear zinc catalysts with unprecedented activities for the copolymerization of cyclohexene oxide and CO2. *Chem. Commun.* **51**, 4579–4582 (2015).
59. Chadwick Ellis, W. *et al.* Copolymerization of CO 2 and meso epoxides using enantioselective β-diiminate catalysts: a route to highly isotactic polycarbonates. *Chem. Sci.* **5**, 4004–4011 (2014).

60. Li, X.-L., Clarke, R. W., Jiang, J.-Y., Xu, T.-Q. & Chen, E. Y.-X. A circular polyester platform based on simple gem-disubstituted valerolactones. *Nat. Chem.* **15**, 278-285 (2022).
61. Matsuo, J., Aoki, K., Sanda, F. & Endo, T. Substituent Effect on the Anionic Equilibrium Polymerization of Six-Membered Cyclic Carbonates. *Macromolecules* **31**, 4432–4438 (1998).
62. Darensbourg, D. J., Moncada, A. I. & Wei, S.-H. Aliphatic Polycarbonates Produced from the Coupling of Carbon Dioxide and Oxetanes and Their Depolymerization via Cyclic Carbonate Formation. *Macromolecules* **44**, 2568–2576 (2011).
63. Darensbourg, D. J., Moncada, A. I., Choi, W. & Reibenspies, J. H. Mechanistic Studies of the Copolymerization Reaction of Oxetane and Carbon Dioxide to Provide Aliphatic Polycarbonates Catalyzed by (Salen)CrX Complexes. *J. Am. Chem. Soc.* **130**, 6523–6533 (2008).
64. Huang, J. *et al.* Selective Organocatalytic Preparation of Trimethylene Carbonate from Oxetane and Carbon Dioxide. *ACS Catal.* **10**, 5399–5404 (2020).
65. Luo, Y.-R. *Comprehensive Handbook of Chemical Bond Energies*. (CRC Press, 2007).
66. Steudel, R. *Chemie der Nichtmetalle: Synthesen - Strukturen - Bindung – Verwendung*. (Walter de Gruyter, 2013).
67. Coates, G. W. & Getzler, Y. D. Y. L. Chemical recycling to monomer for an ideal, circular polymer economy. *Nat. Rev. Mater.* **5**, 501–516 (2020).
68. Darensbourg, D. J., Ganguly, P. & Choi, W. Metal Salen Derivatives as Catalysts for the Alternating Copolymerization of Oxetanes and Carbon Dioxide To Afford Polycarbonates. *Inorg. Chem.* **45**, 3831–3833 (2006).
69. Cao, X. *et al.* Sulfur-substitution-enhanced crystallization and crystal structure of poly(trimethylene monothiocarbonate). *Chin. Chem. Let.* **33**, 1021–1024 (2022).
70. Bhaumik, D. & Mark, J. E. Calculated intermolecular energies relevant to the unusually high melting point of poly(ethylene sulfide). *Macromolecules* **14**, 162–165 (1981).
71. Sasanuma, Y. & Watanabe, A. Conformational Characteristics of Poly(trimethylene sulfide) and Structure−Property Relationships of Representative Polysulfides and Polyethers. *Macromolecules* **39**, 1646–1656 (2006).

TOC Graphic: